MOLECULAR ONCOLOGY 8 (2014) 1603–1615

available at www.sciencedirect.com

ScienceDirect

www.elsevier.com/locate/molonc

Increased sensitivity to ionizing radiation by targeting the homologous recombination pathway in glioma initiating cells

Yi Chieh Lim[a,b], Tara L. Roberts[a,b], Bryan W. Day[a], Brett W. Stringer[a], Sergei Kozlov[a], Shazrul Fazry[a], Zara C. Bruce[a], Kathleen S. Ensbey[a], David G. Walker[c], Andrew W. Boyd[a], Martin F. Lavin[a,b,*]

[a]QIMR Berghofer Medical Research Institute, 300 Herston Road, Herston, Queensland 4029, Australia
[b]The University of Queensland Centre for Clinical Research, Royal Brisbane and Women's Hospital Campus, Herston, Queensland 4029, Australia
[c]BrizBrain and Spine, The Wesley Hospital, Evan Thomson Building, Level 10, Auchenflower, Queensland 4066, Australia

ARTICLE INFO

Article history:
Received 24 March 2014
Received in revised form
20 June 2014
Accepted 20 June 2014
Available online 27 June 2014

Keywords:
DNA damage
DNA double strand break repair
Glioma initiating cell
Neural progenitor cell
ATM inhibitor
Homologous recombination

ABSTRACT

Glioblastoma is deemed the most malignant form of brain tumour, particularly due to its resistance to conventional treatments. A small surviving group of aberrant stem cells termed glioma initiation cells (GICs) that escape surgical debulking are suggested to be the cause of this resistance. Relatively quiescent in nature, GICs are capable of driving tumour recurrence and undergo lineage differentiation. Most importantly, these GICs are resistant to radiotherapy, suggesting that radioresistance contribute to their survival. In a previous study, we demonstrated that GICs had a restricted double strand break (DSB) repair pathway involving predominantly homologous recombination (HR) associated with a lack of functional G_1/S checkpoint arrest. This unusual behaviour led to less efficient non-homologous end joining (NHEJ) repair and overall slower DNA DSB repair kinetics. To determine whether specific targeting of the HR pathway with small molecule inhibitors could increase GIC radiosensitivity, we used the Ataxia-telangiectasia mutated inhibitor (ATMi) to ablate HR and the DNA-dependent protein kinase inhibitor (DNA-PKi) to inhibit NHEJ. Pre-treatment with ATMi prior to ionizing radiation (IR) exposure prevented HR-mediated DNA DSB repair as measured by Rad51 foci accumulation. Increased cell death *in vitro* and improved *in vivo* animal survival could be observed with combined ATMi and IR treatment. Conversely, DNA-PKi treatment had minimal impact on GICs ability to resolve DNA DSB after IR with only partial reduction in cell survival, confirming the major role of HR. These results provide a mechanistic insight into the predominant form of DNA DSB repair in GICs, which when targeted may be a potential translational approach to increase patient survival.

* *Corresponding author*. Radiation Biology and Oncology Laboratory, QIMR Berghofer Medical Research Institute, Locked Bag 2000, 300 Herston Road, Herston, Queensland 4029, Australia. Tel.: +61 7 3362 0341; fax: +61 7 3362 0106.
E-mail addresses: martin.lavin@qimrberghofer.edu.au, m.lavin@uq.edu.au (M.F. Lavin).
http://dx.doi.org/10.1016/j.molonc.2014.06.012
1574-7891/

1. Introduction

Adult neural stem cells (NSCs) are an important component of the mammalian brain required for tissue homoeostasis. Defects in their regulatory mechanisms can contribute to cancer formation. Hence to ensure the different lineages are free from mutagenic inheritances, NSCs (Carlessi et al., 2006; Meletis et al., 2006) and their neural progenitor cells (NPCs) (D'Sa-Eipper and Roth, 2000; Katayama et al., 2005) have a low tolerance or threshold for DNA damage-induced p53-dependent apoptosis.

In spite of the safety mechanisms, mutations do arise in cells with the potential for cancerous growth. A small subset of cancer stem cells (CSCs) similar to NSCs is believed to be responsible for the expansion and cellular differentiation of tumours. Rather than relying on cellular death to preserve genomic integrity, CSCs circumvent apoptosis through efficient DNA repair (Bao et al., 2006). The first documented report supporting this hypothesis came from the isolation of CSCs from GBM tumours. These GIC populations had identical surface marker expression and characteristics to their NSC counterparts (Singh et al., 2003). However, they were more efficient in DNA damage repair (Bao et al., 2006), resulting in a radioresistant phenotype. Current therapy for GBM is to debulk the tumour mass followed by radiotherapy. The initial process often misses the GIC population in the brain (Loeffler et al., 1992; Sanai and Berger, 2008). Residual radioresistant cells continue to propagate after radiotherapy (Tamura et al., 2010), giving rise to tumour recurrences. To limit the progression of tumour growth, pre-clinical and clinical studies suggest an additional chemotherapeutic drug(s) regime to inhibit their DNA repair pathway(s) to increase the response to IR in order to eliminate GIC (Weller et al., 2013).

When GICs acquire DNA damage, cell-cycle arrest is initiated followed by activation of DNA repair pathways. There are two major pathways that repair DNA DSBs; firstly in the NHEJ pathway, the process begins with the binding of Ku70/80 (Ku) proteins with high affinity to the ends of the DNA termini in a structure-specific manner followed by the recruitment and activation of DNA-dependent protein kinase catalytic subunit (DNA-PK_{cs}). Together with the Artemis protein, damaged DNA is then processed and the ligase IV-XRCC4 complex is recruited to join the DNA ends together (Goodarzi et al., 2006). HR is the second major pathway for DNA DSB repair. In the presence of DNA damage, the Mre11/Rad50/Nbs1 (MRN) complex recruits and activates ATM and other DNA damage response proteins to the DNA termini (Lavin, 2008). MRN initiates early DNA processing that is subsequently promoted by CTBP-interacting protein (CtIP) (Limbo et al., 2007). Other proteins such as exonuclease 1 (Exo1) and DNA replication helicase 2 homolog (Dna2) have also been implicated to resolve the DSB that is required to create 3′-single strand (ss)-DNA (Nicolette et al., 2010). The resulting 3′-overhang is stabilised by replication protein A (RPA), which is subsequently displaced by Rad51 to form nucleoprotein filaments for invasion and searching for complementary sequences on the sister chromatid to achieve template duplication and repair (Escribano-Díaz et al., 2013).

The types of DNA processing occurring during the different cell-cycle stages (Allen et al., 2003; Mao et al., 2008) are critical determinants governing the choice between the two DNA repair pathways (Escribano-Díaz et al., 2013). For instance, both the MRN complex and the Ku heterodimer bind almost instantaneously upon sensing damaged DNA. However, extensive resection is facilitated during S- and G_2-phase of the cell-cycle in an MRN-Sae2/CtIP dependent manner to create a DNA substrate less suitable for Ku heterodimer binding thus committing cells to HR (Huertas and Jackson, 2009). Whereas in G_1-phase of the cell-cycle resection is less active and the situation favors Ku heterodimer binding to DNA ends, suppressing initiation of resection. The process then mediates recruitment of other NHEJ factors. Due to the competition for damaged DNA substrates, HR and NHEJ have overlapping roles (Takata et al., 1998). Recent work has also shown that BRCA1 and 53BP1 play essential roles in the promotion of HR or NHEJ respectively (Tang et al., 2013). Specifically histone acetylation at the break site determines the balance of BRCA1 and 53BP1 at the DNA-DSB by altering 53BP1 binding affinity and increasing BRCA1 loading, promoting HR. Similarly, lack of MRN complex or Sae2 results in a better access of Ku heterodimer binding to DNA ends, thus increasing NHEJ (Clerici et al., 2008). By contrast, deficiency in Ku heterodimer increases DNA resection and ultimately drives HR repair (Langerak et al., 2011).

The redundancy of multiple pathways plays a vital role in cell survival. Without an efficient DSB repair mechanism, the overall DNA damage can trigger cell death. In our previous study, we demonstrated that GICs preferentially used the less error-prone repair pathway, HR (Lim et al., 2012). Considering that NHEJ is the predominant repair pathway in non-tumourgenic NPCs, the data suggested that GICs would be targeted by drugs inhibiting the HR pathway (Short et al., 2007). This hypothesis was also supported by our finding that siRNA knockdown of Rad51 significantly increased the radiosensitivity in GICs. The requirement for ATM in HR repair (Beucher et al., 2006), led to earlier studies on radiosensitising cells with non-specific phosphoinositide 3 kinase like-kinase (PIKK) inhibitors; wortmannin and caffeine (Sak et al., 2005; Wang et al., 2003). Although ATM phosphorylation was diminished, a number of PI3K members including DNA-PK_{cs} were also targeted (Sarkaria et al., 1998). Herein, we demonstrate the use of a specific small molecule ATM kinase inhibitor in combination with IR to target GIC (Hickson et al., 2004; Hosoya and Miyagawa, 2009). The data show that by inhibiting HR specifically, GIC can be radiosensitised while surrounding normal neural tissue is protected through NHEJ to maintain survival.

2. Material and methods

2.1. *Glioma initiating and neural stem cell maintenance*

Neurosphere lines were maintained as suspension cultures at 37 °C in 5% CO_2 with growth supplements as described previously (Reynolds and Weiss, 1992). Three primary human-derived (L2b, L3b and Wk1) and one ATCC (U251) GBM

neurosphere lines used in this study were obtained from Day et al. (Day et al., 2013, 2011). A commercially available non-tumourgenic NPCs or ReNcell (Millipore, USA) derived from fetal brain tissue was also included in this study (Donato et al., 2007). Neurospheres were trypsinised into single cell suspensions prior to experimentation.

2.2. Chemicals

The compounds, ATMi (ATM kinase inhibitor), 2-Morpholin-4-yl-6-thianthren-1-yl-pyran-4-one (Ku55933) (Hickson et al., 2004) and DNA-PKi (DNA-Pk_{cs} kinase inhibitor), 1-(2-Hydroxy-4-morpholin-4-yl-phenyl)-phenyl-methanone (AMA37) (Sturgeon et al., 2006) were purchased from Calbiochem, USA. Both drugs were prepared as 10 mM stock solutions in DMSO. For all drug treatments, cells were pre-incubated with the indicated concentration for 1 h prior to irradiation.

2.3. Irradiation

Single cells dissociated from neurospheres were irradiated with a 137Cs gamma rays source at a dose rate of 1.12 Gy/min for 107 s which is the equivalent of 2Gy (MDS Nordion Gammacell Irradiator).

2.4. Cell survival assays

Cell survival was determined either by trypan blue exclusion or clonogenic assay as described previously by Lim et al. (2012) and Franken et al. (2006) respectively. In the latter, a single cell suspension was treated with the respective inhibitors followed by irradiation. Cells were plated 2 h later onto Matrigel™ (Becton Dickinson, USA) coated-plate and fixed with 1% formaldehyde in methanol at 96 h post-treatment. Clonogenic growth was determined by measuring the absorbance of solubilised crystal violet colonies in 10% acetic acid.

2.5. Protein extracts and immunoblotting

Neurosphere cultures were centrifuged, harvested and resuspended in lysis buffer as described (Lim et al., 2012). For immunoblotting, protein extracts (40 μg) were electrophoresed on 4%–12% NuPAGE® Bis-Tris (Invitrogen, USA) gels before transferring onto nitrocellulose membrane Hybond-C (Amersham Biosciences, UK). Membranes were blocked overnight in PBS/0.02% Tween-20 containing 5% skim milk, followed by incubation with the various antibodies as detailed below. Immunoblotting was performed as described previously (Roberts et al., 2013).

2.6. The primary antibodies and their respective dilutions for immunoblotting

Anti-phospho^{Ser1981} ATM (1:2000, R&D system, USA), anti-ATM (1:2000, GeneTex®, USA), anti-phospho^{Ser516} Chk2 (1:1000, Cell signaling, USA), anti-Chk2 (1:1000, Cell signaling, USA), anti-PCNA (1:2000, Oncogene, USA), anti-Rad51 (1:1000, Santa Cruz, USA) and HRP-linked secondary antibodies (1:5000, Sigma-Aldrich, USA).

2.7. Cell-cycle analysis

Asynchronous single cells were pre-treated with 5 μM ATMi for 1 h before irradiation and harvested at various time points. Cells were then fixed with 70% ethanol and stored at −20 °C for 24 h before analysis. Approximately 1×10^6 cells were incubated with 30 μg of propidium iodide (PI) (Sigma-Aldrich, USA) per ml, and DNA content was measured by flow cytometry (FACScan, Becton Dickinson, USA). Data were analysed with Modfit® software.

2.8. Mitotic assay

Drug and irradiation dose treatment were performed as described in cell-cycle analysis. Cells were then fixed with 70% ethanol and stored at −20 °C for 24 h. Fixative solution was removed the next day before resuspending in PBS solution containing 0.2% Triton X-100 and 5% BSA. Samples were immunostained with Alexa488-conjugated anti-phospho^{Ser10} histone H3 (Cell signaling, USA) as per manufactures protocol (Sturgeon et al., 2006). Data were analysed with CellQuest® software.

2.9. Immunofluorescent labelling and DNA damage repair kinetic studies

The assay was previously described (Wang et al., 2003) with minor modification. Briefly, cells were harvested and fixed with 2% PFA on ice, resuspended in PBS and stored overnight at 4 °C. Approximately 1×10^4 cells were cytocentrifuged (Shandon, USA) at 600 g for 15 min onto Superfrost® plus slides (Menzel-Gläser, Germany). Immunostaining for γH2AX was performed as described previously (Langerak et al., 2011). For Rad51 analysis, slides were blocked with 5% BSA in 0.5% Triton X-100/PBS at room temperature prior to adding 1:100 anti-Rad51 in 2% BSA/PBS followed by secondary antibody 1:250 (Alexa488, Invitrogen, USA) and 1:10,000 Hoechst stain. All slides were mounted with ProLong® Gold (Invitrogen, USA) before viewing on a DeltaVision fluorescence microscopy system (Applied Precision) with a 60×/1.4 Olympus Plan-APOCHROMAT oil lens. Images were acquired with Softworx imaging software (Applied Precision).

2.10. Evaluation of tumourigenicity by intracranial injection

Primary Wk1 GIC line with a stable integrated luciferase tag (Wk1-luc) was established as described previously (Day et al., 2013). To determine the efficacy of DNA repair inhibition and its role in promoting animal survival, Wk1-luc was treated with the different respective inhibitors prior to 2Gy IR treatment. Cultures were harvested 48 h later and trypsinised into single cell suspensions in DPBS. Approximately 1.5×10^5 live cells were intracranially injected into the right hemisphere of each mouse with the following coordinates; Posteroanterior = −1.2 mm from bregma, Mediolateral = +0.6 mm from midline, Dorsoventral = −3 mm using a stereotactic device. Mice were then allowed to develop tumours for 6–16 weeks. Upon onset of symptoms (hunching, weight loss, and rough coat) mice were sacrificed, tumour samples taken, formalin fixed, embedded and analysed by haematoxylin and eosin staining.

2.11. Statistic analysis

Where indicated, all presented data are pooled from three independent experiments and represented as mean ± SD. Student's *t*-test (one-tail, with equal sample and variance) was performed in Microsoft excel 2008. Single asterisk represents a p-value of <0.05, whereas two asterisks a p-value of <0.01.

3. Results

3.1. Non-homologous end joining is not a major repair pathway in glioma initiating cells

We previously demonstrated that HR rather than NHEJ was the key pathway involved in GIC DNA DSB repair (Lim et al., 2012). For this reason, we proposed that targeting HR might provide a method to increase the efficacy of IR against GBM treatment. To investigate this possibility, we employed commercially available drugs; ATMi to ablate HR activity and DNA-PKi to disrupt NHEJ-mediated repair. We previously titrated DNA-PKi at various concentrations and found that 30 μM was sufficient to inhibit >50% of DNA-PK_{cs} autophosphorylation (Brown et al., 2011). A similar approach was also conducted with ATMi and identified 5 μM as optimal with the least effect on cell viability (Figure 1A). Treatment at this concentration prior to 2Gy IR prevented ATM autophosphorylation on serine 1981 and inhibited downstream activation of the ATM substrate, Chk2 (Figure 1B). Lymphoblastoid cells harvested from Ataxia-telangiectasia (A-T) patients are incapable of eliciting cell-cycle checkpoints after IR and at later times accumulate in G_2/M phase (Beamish and Lavin, 1994). When treated with ATMi alone, the inhibitor did not modulate cell-cycle distribution (Figure 1C). However, exposure to 2Gy IR showed changes in the cell-cycle profile with almost equal distribution of asynchronous cells between G_1 (38.15%) and G_2 (34.98%), indicating checkpoint activation is present in the respective cell-cycle phases (Figure 1C). When treated with ATMi prior to 2Gy IR, cells displayed hallmarks of A-T with a greater number accumulating in G_2-phase (54.85%) (Xu et al., 2002). Measurement of phosphorylation of ^{S10}Histone H3 (mitotic marker) confirmed that ATMi treatment prior to IR failed to reduce the rate of G_2-phase cells entering mitosis (Figure 1D). In the absence of ATMi, functional ATM activation following IR prevented entry of G_2-phase cells into mitosis (Figure 1E).

To investigate NHEJ-dependent repair after IR-induced damage in the presence of the different inhibitors, we transiently transfected both non-tumourigenic NPCs and GICs with a linearised pEGFP plasmid. Due to the introduction of a 'DSB' via endonuclease excision between the promoter and gene, endogenous GFP expression is only possible after DNA repair. NHEJ activity was allowed to proceed for 48 h before samples were subjected to flow cytometry analysis (Supplementary Figure 1A). For DMSO treatment prior to transfection, NHEJ repair efficiency was 51.55% in NPC with 23.39% and 26.50% in the GIC lines; U251 and L2b respectively (Supplementary Figure 1B). Following pre-treatment with DNA-PKi, NHEJ repair was reduced to 37.11% in NPC while efficiency in the GICs were 13.53% in U251 and 11.36% in L2b.

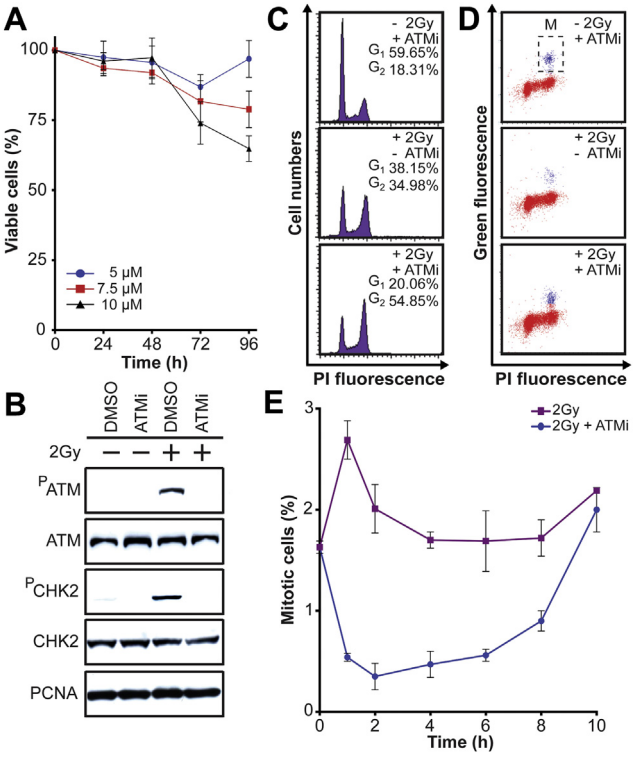

Figure 1 – The effect of ATM inhibition on glioma initiating cells. (A) Cell viability was measured by trypan blue exclusion assay. The difference in cell count at each time point was normalised back to its own individual unirradiated sample. ATMi concentration was chosen based on the least cytotoxic effect. Data show the mean from a combination of three independent experiments and error bars display the standard deviation (±SD). (B) 5 μM ATMi was validated by examining the activation of ATM as measured by autophosphorylation of Serine 1981 and the ATM substrate Chk2 at Serine516 in response to IR. Cells were treated with or without inhibitor for 1 h prior to irradiation and harvested post-IR 1 h later. (C) Cells were harvested at 16 h and stained with PI to measure cell-cycle progression. *X*-axis indicates fluorescence intensity of PI and *Y*-axis measures the total cell number. (D) Asynchronous cells were pre-treated with 5 μM ATMi prior to IR. The cells were fixed, harvested and immunostained for ^{Ser10}Histone H3 and PI dye. *X*-axis represents mean fluorescence intensity of PI and the *Y*-axis ^{Ser10}Histone H3 Alexa 488 nm fluorescence. (E) Quantification of the total number of mitotic cells as determined by ^{Ser10}Histone H3 staining. Data are pooled from two independent experiments and represented as mean ± SD.

Both NPCs and GICs treated with ATMi had relatively unchanged NHEJ repair efficiency compared to their DMSO treated samples. ATMi at this concentration (5 μM) is non-specific to NHEJ inhibition.

3.2. ATM-dependent homologous recombination is crucial in glioma initiating cell DNA DSB repair

We next examined the kinetics of cells with Rad51 foci, a marker for HR initiation and resolution. Irradiation of both

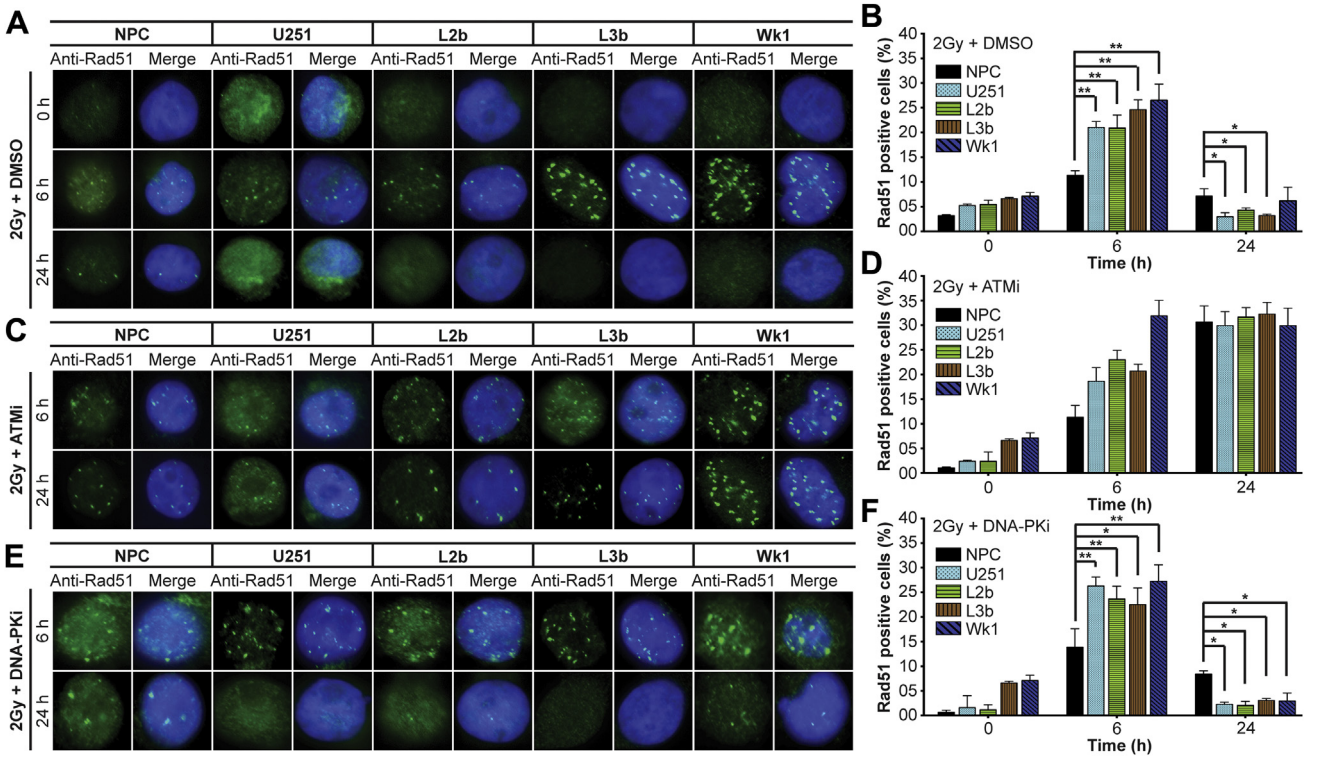

Figure 2 – Rad51 foci accumulation post-IR is enhanced by ATMi treatment of GICs and NPCs. Cells were treated with (A) DMSO, (C) ATMi or (E) DNA-PKi prior to 2Gy IR, harvested at the indicated times and then immunolabelled to detect Rad51 foci (green). Representative images for each time point show Rad51 foci and Hoechst nuclear stain (blue). (B), (D) and (F) Quantification of Rad51 positive cells was determined by a nucleus with >5 foci. Data show the mean from a combination of three independent experiments and error bars display the ±SD (*$p < 0.05$, **$p < 0.01$).

NPCs and GICs induced Rad51 foci formation at 6 h (Figure 2A) but the number of cells positive for Rad51 foci undergoing HR was significantly less in NPCs (Figure 2B). At 24 h, the number of Rad51 foci positive cells was resolved across all GIC lines (2.96% in U251, 4.34% in L2b, 3.20% in L3b and 6.18% in Wk1) when compared to NPC (7.16%) (Figure 2A, B). When treated with ATMi prior to IR, the percentage of cells with Rad51 foci was similar to irradiated only cells at the 6 h time point (Figure 2C, D). NPC had 11.32% Rad51 foci positive cells, while U251, L2b, L3b and Wk1 had 18.63%, 23.05%, 20.69% and 31.91% respectively. At 24 h, the level of Rad51 foci positive cells continued to increase in all neurosphere lines and was comparable between NPCs (30.65%) and GICs (U251 – 29.93%, L2b – 31.66%, L3b – 32.26% and Wk1 – 29.92%), indicating HR inhibition in both cell types. To further validate the specificity of Rad51 foci as a marker of HR, we employed the use of a cell-cycle marker that is regulated in S- and G_2-phase (BrdU) (Terry and White, 2006). At 24 h post-treatment, we observed Rad51 foci expression only in BrdU positive cells (Supplementary Figure 2A). There was a lack in resolving Rad51/BrdU positive cells (L3b – 24.62% and Wk1 – 26.72%) when given ATMi prior to irradiation (Supplementary Figure 2B). Both pieces of data (Figure 2D and Supplementary Figure 2B) demonstrate similar outcomes supporting the specificity of ATMi in HR repair inhibition. In DNA-PKi pre-treated samples following 2Gy IR, the inhibitor did not affect HR repair kinetics. Rad51 foci formation and resolution showed similar DNA DSB recovery to irradiated only samples (Figure 2E and Supplementary Figure 2B). At 24 h, samples that received DNA-PKi in combination with 2Gy IR showed a return to basal level with Rad51 foci in 2.28% (U251), 2.05% (L2b), 3.08% (L3b), 2.94% (Wk1) and NPC (8.42%) of cells (Figure 2F).

We next confirmed the effect of ATMi treatment on HR efficiency using a DNA DSB repair reporter assay. Neurosphere lines containing an integrated HR reporter (pDR-GFP) were generated as described previously (Allen et al., 2003). This was followed by I-SCE I endonuclease expression vector transfection to introduce a single DSB within the HR reporter construct to initiate recombinant DNA repair. Similar to NHEJ, HR repair was allowed to progress for 48 h prior to flow cytometry analysis (Supplementary Figure 3A). Without inhibitor (DMSO alone), HR repair in the U251 and L2b GIC lines was 3.76% ($p < 0.01$) and 3.92% ($p < 0.01$) respectively. NPCs on the other hand had 0.66% of HR repair (Supplementary Figure 3B). However, with the addition of ATMi, HR efficiency was reduced in both NPCs (0.17%) and GICs; U251 (1.09%) and L2b (0.62%). Immunoblot analysis of repair proteins required for HR (Rad51, ATR, and ATRIP) showed no increase in protein level (GICs versus NPCs) (Supplementary Figure 3C). The collated data suggest that mechanistic selection rather than protein levels in the HR pathway is different between NPCs and GICs.

3.3. *Homologous recombination inhibition compromises overall DNA DSBs repair in glioma initiating cells*

Since γH2AX foci mark all DNA DSBs, we next sough to determine the overall effect of the different inhibitors on DNA repair and whether one pathway could compensate for the other when specifically inhibited. When given irradiation only, maximum DNA damage levels induced in U251, L2b, L3b and Wk1 (Figure 3A) at 1 h were 32, and 24, 25 and 38 foci per cell respectively. Although the γH2AX (22 foci per cell) level in NPC was less (Figure 3B), DNA DSB repair was more rapid with a return to basal level after 12 h (3 foci per cell). At the same time point (12 h), residual DNA breaks were still present in significant numbers across all GICs (U251 – 13 foci per cell, L2b – 6 foci per cell, L3b – 10 foci per cell and Wk1 – 12 foci per cell), which only achieved complete DNA DSB repair by 24 h (between 1 and 6 foci per cell).

When treated with DNA-PKi prior to 2Gy IR (Figure 3C, D), all samples reached a maximum number of γH2AX foci comparable to their irradiated only (DMSO) controls at 1 h (Figure 3B) – 23, 32, 26, 25 and 40 foci per cell in NPC, U251, L2b, L3b and Wk1 respectively. An increase in unresolved breaks (20 foci per cell) at 12 h suggested less efficient DNA DSB repair in NPC (Figure 3D) with minimal resolution of DNA damage even after 24 h (16 foci per cell). In L2b and L3b, DNA-PKi treatment prior to 2Gy IR resulted in only a slight delay to γH2AX foci resolution. Although at 12 h the DNA damage was higher than its own irradiated only sample (DMSO) (13 versus 6 foci per cell in L2b and 16 versus 5 foci per cell in L3b), considerable DNA DSB repair was achieved by 24 h with a return to basal level (6 and 5 foci per cell in L2b and L3b, respectively) ($p < 0.01$) as compared to NPC (Figure 3D). In U251 and Wk1, there were no statistical differences between the γH2AX foci numbers observed at 12 h in DNA-PKi treated and DMSO treated samples (14 versus 13 foci per cell in U251 and 16

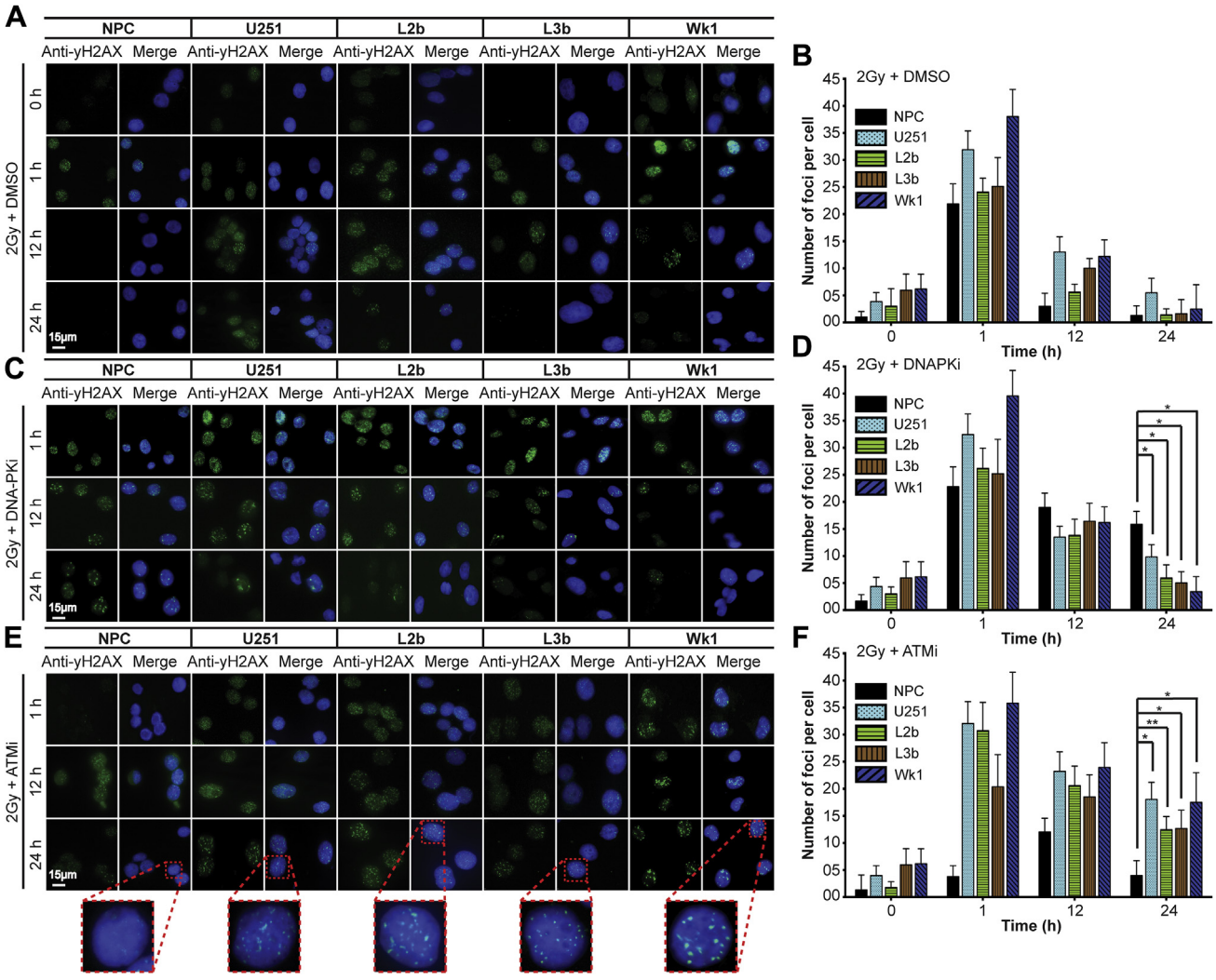

Figure 3 – ATMi-treated GICs are unable to compensate for IR-induced DNA damage through the NHEJ pathway. Cells were treated with (A) DMSO, (C) DNA-PKi or (E) ATMi for 1 h prior to 2Gy IR, harvested and immunolabelled at indicated time points. Representative images of NPCs and GICs with γH2AX foci formation (green) and Hoechst nuclear stain (blue). (B), (D) and (F) Each time point, the average foci number was scored from approximately 40 nuclei per experiment. Data show the mean from a combination of three independent experiments and error bars display the ±SD (*$p < 0.05$, **$p < 0.01$).

versus 12 foci per cell in Wk1). At 24 h post-2Gy IR, residual γH2AX foci for U251 with and without DNA-PKi treatment were 10 and 5 foci per cell respectively. Similar results were observed in Wk1 (post-24 h) receiving either DNA-PKi with irradiation (2 foci per cell) or irradiated only (DMSO) (3 foci per cell). The DNA-PKi data set was not significantly different to the irradiated only (DMSO) group, suggesting a limited role for DNA-PK_{cs} in DNA DSB repair in GIC (Figure 3D).

In ATMi-treated NPCs prior to 2Gy IR, the number of γH2AX foci was 4 foci per cell (at 1 h) (Adams et al., 2010a; Hickson et al., 2004) and continued increasing at 12 h (12 foci per cell) (Figure 3E, F). By 24 h, NPCs had resolved the majority of DNA DSBs (4 foci per cell). While ATMi did not ablate γH2AX phosphorylation at 1 h in GICs, DNA DSB repair slowed considerably. At 12 h, the level of γH2AX foci formation was 23, 21, 19 and 24 foci per cell in U251, L2b, L3b and Wk1 respectively (Figure 3E). Foci numbers showed modest decrease at 24 h in U251 (18 foci per cell), L2b (12 foci per cell), L3b (13 foci per cell) and Wk1 (17 foci per cell). An independent analysis using an alternate DNA DSB marker (53BP1) (Asaithamby and Chen, 2009) was also employed to confirm the effect of DNA-PKi and ATMi in GIC (Supplementary Figure 4A–C). Similar to γH2AX kinetics, GICs that received treatment with DNA-PKi or DMSO prior to 2Gy IR showed comparable repair of DNA DSB (2–4 foci per cell) by 24 h (Supplementary Figure 4D, E). Conversely when given ATMi prior to IR, a significant delay in repairing DNA DSB was observed. Residual DNA DSB damage in GICs was approximately 15 foci per cell ($p < 0.01$) (Supplementary Figure 4D, E). From the observed data, the presence of ATMi prior to irradiation limits active DNA DSB repair in GIC.

3.4. *GIC requires homologous recombination repair after IR for survival*

We next determined if GIC survival following IR was dependent on DNA DSB repair via either NHEJ or HR. In irradiated only cells (DMSO alone), all GIC demonstrated approximately the same viability throughout the entire time course and by 96 h had 52.50% (U251), 46.26% (L2b), 49.43% (L3b) and 66.02% (Wk1) cell survival. NPC on the other hand had 21.09% viable cells at 96 h, which was significantly lower that in GICs ($p < 0.01$) (Figure 4A). Treatment with DNA-PKi prior to IR did not significantly affect the overall survival of GICs (Figure 4A). By 96 h, a modest decrease in survival was observed in U251 (46.94%), L2b (38.17%), L3b (45.01%) and Wk1 (54.62%). However, NPC survival was markedly reduced by DNA-PKi pre-treatment. Viable cells were reduced to 35.34% at 24 h and continued to decrease throughout the time course. By 96 h, NSC had 11.24% viable cells. The data indicated NHEJ inhibition had minimal effect on GIC recovery from IR-induced DNA damage but a strong impact on NPCs survival. When given ATMi prior to IR, the viability of the GICs decreased dramatically (Figure 4A) with similar survival to NPCs observed from 72 h onwards (NPC – 13.22%, U251 – 22.66%, L2b – 21.34%, L3b – 23.60%, and Wk1 – 21.61%). This data set indicates that ATMi sensitised GICs to a greater degree than NPCs, thus supporting the reliance on HR for GICs.

To explore further the effect of DNA-PKi and ATMi on GIC's survival, we examined the effect of the different inhibitors on colony formation. Post-96 h, GICs that received only 2Gy IR showed modest growth inhibition despite IR-induced DNA damage insults. Absorbance readings based on crystal violet stain intensity indicated higher cell proliferation (U251 – 80.82%, L2b – 78.72%, L3b – 88.24% and Wk1 – 90.66%) compared to NPC (51.16%) (Figure 4B, C). When given DNA-PKi prior to 2Gy IR, a decrease in cell growth was observed in NPC (37.82%). In contrast, DNA-PKi in combination with 2Gy IR caused minimal growth reduction in GICs. Surviving fractions across the different GIC lines (U251 – 73.52%, L2b – 69.79%, L3b – 82.12% and Wk1 – 87.29%) remained similar to their irradiated only (DMSO) counterparts. GICs growth reduction occurred after treating ATMi prior to 2Gy IR (Figure 4C). At 96 h post-treatment, cell survival was reduced to 19.57%, 10.40%, 8.79% and 11.63% in U251, L2b, L3b and Wk1 respectively. These data reveal a significant role for ATMi in radiosensitising GICs by inhibiting HR repair.

Based on the neurosphere assay that quantifies the size of cell clusters (spheres) from individual cells with long-term growth potential, the degree of radiosensitisation of GICs to ATMi and 2Gy IR treatment combination was comparable to a total dose of 10Gy alone (Supplementary Figure 5A). These data further illustrate the radioresistant properties of GICs and the important role for HR in protecting these cells against radiation-induced cell death (Supplementary Figure 5B).

3.5. *ATMi treatment prior to ionizing radiation increases survival in tumour-bearing animals*

As a proof of principle that HR repair inhibition is a viable therapeutic option for GBM treatment, we assessed the tumourigenic potential of a primary pre-treated luciferase-tagged GICs (Wk1-luc) in NOD/SCID mice. Four different treatment groups (DMSO, 2Gy IR, DNA-PKi or ATMi in combination with 2Gy IR) received equal numbers of intracranially injected Wk1-luc cells. Tumour quantification was based on the bioluminescence intensity of Wk1-luc cells (Figure 5A). In DMSO treated animals, the average median survival time was 94 days followed by 2Gy IR treated animals (101 days) and the pre-treated DNA-PKi with 2Gy IR group (104 days) (Figure 5B). There was no statistical significance between these three cohorts. Treatment with ATMi and 2Gy IR on the other hand had a greater effect on Wk1-luc proliferation. Marked improvement could be identified with a median animal survival of 130 days ($p < 0.05$) (Figure 5B). The development of GBM tumour in each cohort was confirmed by H&E staining of brain sections (Figure 5C) except for one animal from the ATMi and 2Gy IR cohort at day 98 which showed absence of brain tumour formation. Overall, the data demonstrate clearly the inefficacy of IR-induced cell death in GIC which can be overcome by the prevention of HR repair through ATM inhibition.

4. Discussion

To date, more than half of all patients diagnosed with cancer undergo some form of radiotherapy with varying success (Siegel et al., 2012). Early stages of cancer are generally more receptive to radiation treatment giving rise to higher survival

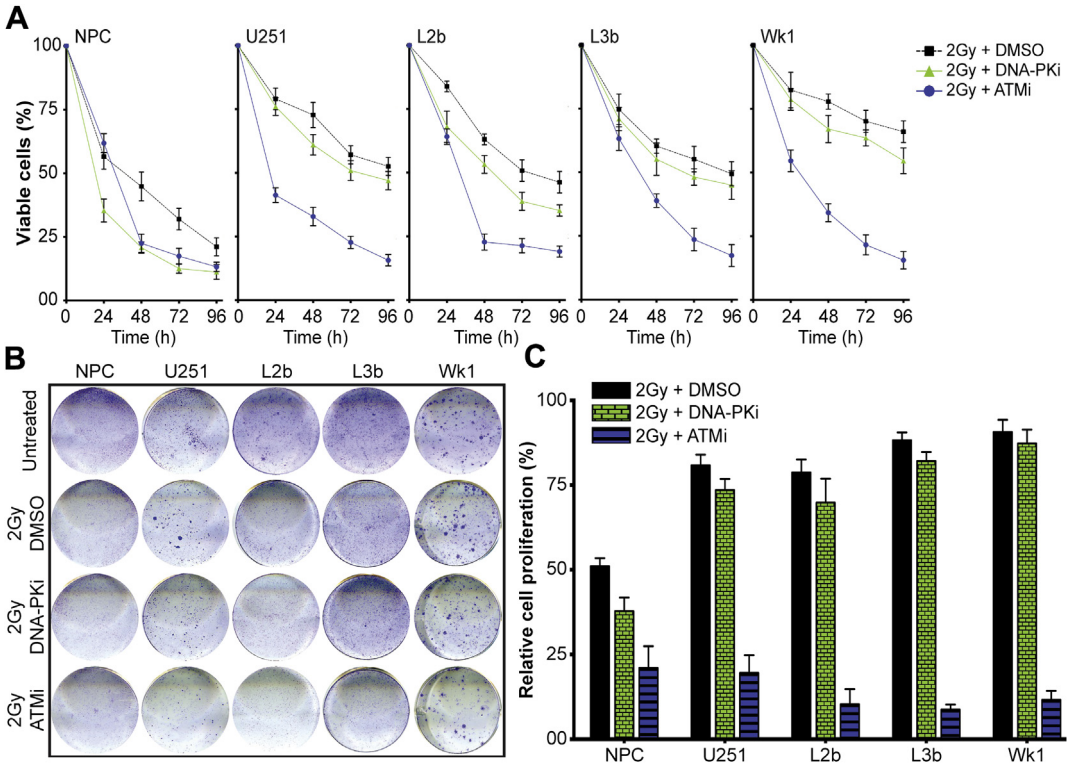

Figure 4 – GICs are dependent on HR-mediated repair for survival. (A) Cells were pre-treated with DMSO, ATMi or DNA-PKi for 1 h prior to IR. Survival of cells was determined by trypan blue exclusion assay at the indicated time points. Data are presented as mean from three independent experiments. (B) Clonogenic assay was performed at 96 h post-treatment with the indicated inhibitors followed by 2Gy IR. Cells were stained with crystal violet to visualise colonies. (C) Cell density is proportionate to the intensity of crystal violet stain. Cell survival was determined by measuring the absorbance of crystal violet stain from individual wells. Data show the mean from a combination of three independent experiments and error bars display the ±SD.

rates. Late stage cancers are refractory to radiotherapy and only short-term benefits result without complete disease regression (Lomonaco et al., 2009; Tamura et al., 2010). At the malignant stage of disease, the average survival for GBM patients undergoing surgical resection in combination with radio- and chemotherapy is approximately two years. Malignancies associated with genetic mutations are believed to be the cause of radiation resistance, potentially through extended use of alternative DNA repair pathway(s). Hence cancer cells have better survival after treatment and result in a poorer prognosis for the patients (Tamura et al., 2010). Mutations which alter signalling pathways may result in differences in DNA damage responses between cancer cells and normal tissue that allow for selective targeting of the tumour (Meador et al., 2010; Short et al., 2011). In a previous report, we demonstrated the use of DNA DSB repair pathways in non-tumourgenic NPCs and tumourgenic GICs (Lim et al., 2012). Most committed cell types, including NPCs, when sensing DNA damage induce cell-cycle arrest at G_1/S-phase to allow the NHEJ pathway to initiate DSB repair (Adams et al., 2010b; Beucher et al., 2006). In GICs, there was a defective cell-cycle arrest at this checkpoint and less reliance on NHEJ repair pathway following DNA damage (Lim et al., 2012). In contrast, functional G_2 cell-cycle arrest was present to allow HR-mediated repair to occur.

A similar phenomenon involving HR repair was identified in mammalian embryonic stem (ES) cells where the G_1/S checkpoint was absent (Adams et al., 2010a; Tichy et al., 2010). Possibly in the small stem cell population, it is crucial for damaged DNA to be repaired with minimal residual mutations rather than having a low tolerance to DNA damage initiated cell death. In agreement, animal models deficient in key HR pathway proteins died from chromosomal aberrations during early embryonic (e5.5) stages (Tsuzuki et al., 1996). Conversely, in an animal model of NHEJ deficiency lethality occurred much later in embryonic development (e16.5) (Karanjawalaa et al., 2002). Another plausible explanation as to why HR is more crucial in ES cells, is the greater number of cells cycling through S-phase as compared to a more committed cell lineage (Fluckiger et al., 2005). The finding with ES cells bears resemblance to the cell-cycle defect in GIC, where there is a lack in G_1/S arrest and a higher proportion of S-phase cells (Lim et al., 2012).

In an attempt to increase radiosensitivity of GIC, we exploited this unusual behaviour where these cells continued to enter S-phase and initiate HR repair post-irradiation by inhibiting the activity of ATM, a key protein in this process (Lim et al., 2012). The strategy increases IR efficacy through specific HR inhibition to enhance DNA damage in cancer cells while limiting the effect on surrounding normal tissue. In this

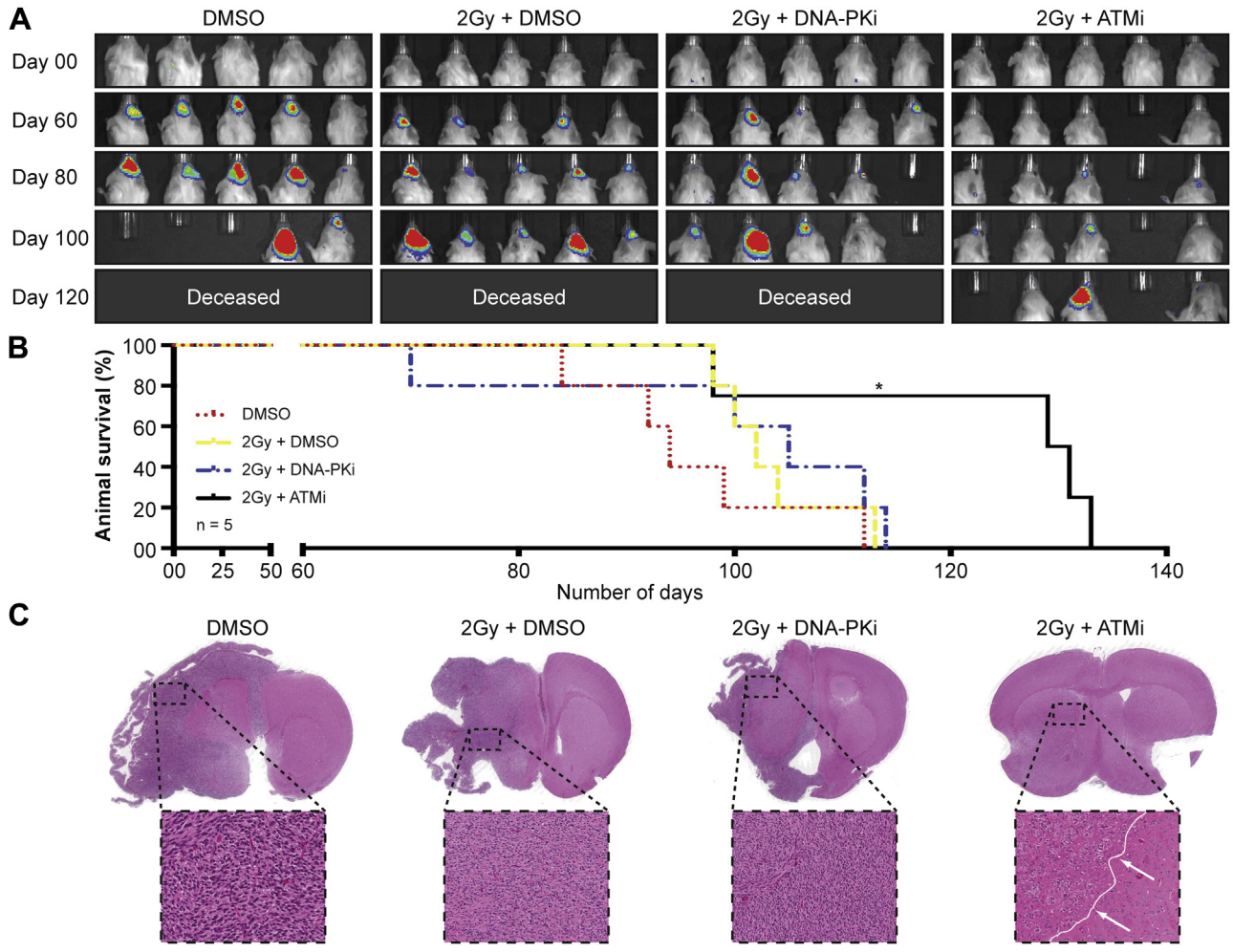

Figure 5 – ATMi treatment prior to ionizing radiation increases the survival of tumour bearing animals. (A) Wk1-luciferase tagged cells were pre-treated with DMSO, DNA-PKi or ATMi for 1 h prior to 2Gy IR. Live cells were determined by trypan blue exclusion assay 48 h later followed by intracranial injection of equal numbers of cells. Image shows the progression of tumour growth in Nod/Scid mice. (B) Kaplan–Meier survival plot showing survival of mice from the individual treated groups ($n = 5$) (*$p < 0.05$). (C) Coronal plane sections of mouse brains injected with Wk1-luciferase tagged cells that received DMSO, DNA-PKi or ATMi in combination with 2Gy IR treatment. Photomicrographs (10× magnification) of H&E stained sections showed dense cellularity of neoplastic cells with invasive growth. White line with indicated arrows (far right panel) shows partial indistinctive border of early tumour progression in 2Gy + ATMi treated group.

case, the lack of, or reduced NHEJ activity would prevent GICs from compensating for the loss of HR through ATMi, resulting in unrepaired damage and cell death. Conversely, NPCs should have better comparable survival because of their limited reliance on HR and the fact that NHEJ-mediated repair is still the primary pathway to combat radiation-induced DNA DSB. The method is analogous to a synthetic lethal approach where lesions generated by inhibition of one pathway are rendered lethal by obstructing the other (Nijman and Friend, 2013).

Depending on the source of the lesions generated, HR can be activated by either ATM-dependent DNA DSB signalling pathways or ATR-directed ATM signalling (Li and Heyer, 2008; Sirbu et al., 2011). However, ATM can also play a role in activating the NHEJ pathway in GICs. We acknowledged that inhibition of ATM might not target HR solely. However, a previously described ATMi study had demonstrated that moderate or low dose of ATMi had no effect on the NHEJ pathway (Brown et al., 2011; Patel et al., 2011). We used 5 μM ATMi, a 50% reduction from the recommended dose for this study (Hickson et al., 2004). At this concentration, autophosphorylation of ATM was eliminated, along with downstream substrate Chk2 inactivation with minimal cytotoxic effect. Based on the current concentration of the inhibitor, it was sufficient to establish a classic A-T phenotype including delay in G_2 cell-cycle arrest and unperturbed mitotic entry. When we compared IR-treated GIC in the presence or absence of ATMi, the former treatment showed no significant changes in NHEJ repair despite a 3–4 fold reduction in HR efficiency being observed in the pDR-GFP repair assay. The data clearly demonstrate the specificity of ATMi for HR inhibition. Examination of Rad51 foci formation also confirmed the decrease in repair via HR. Immunoblot analysis of key proteins involved in HR (ATR, ATRIP and Rad51) on the other hand ruled out

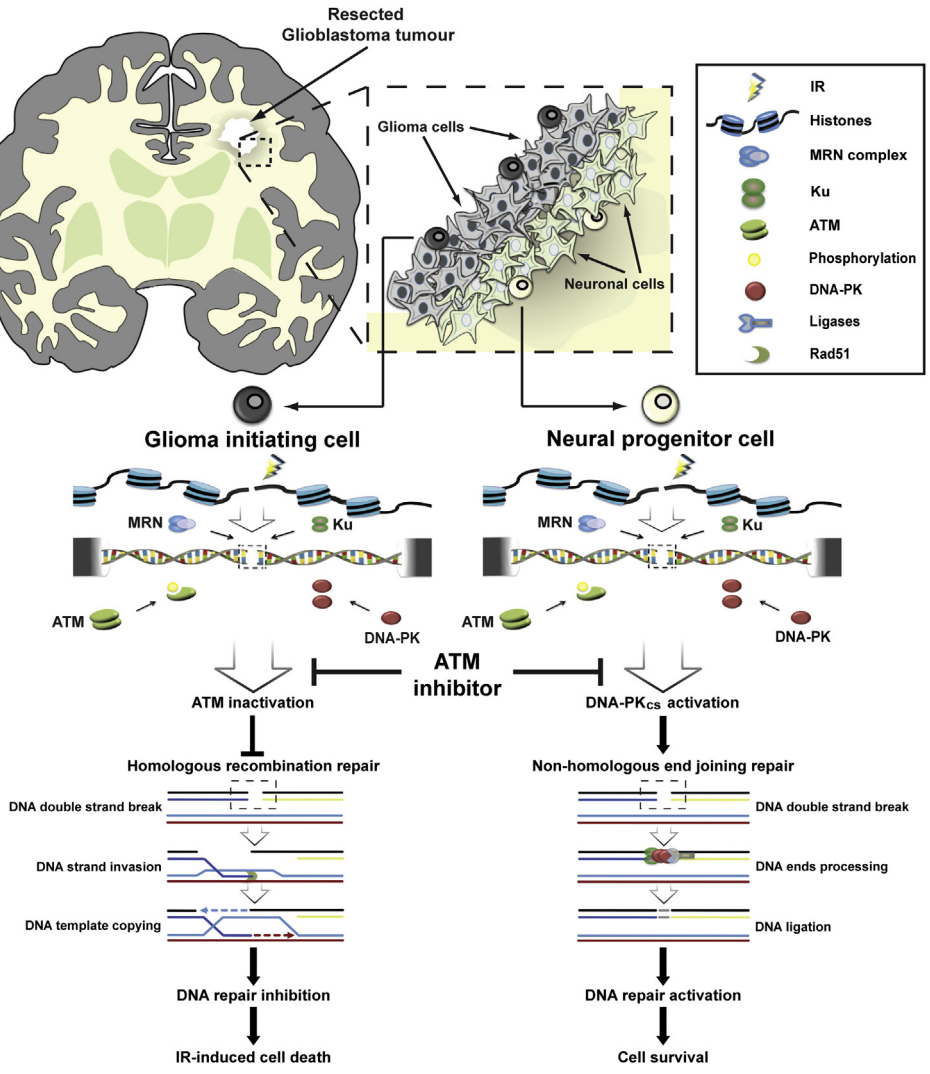

Figure 6 – A simplified model for the effect of ATM inhibitor on GICs which have limited NHEJ repair. Post-surgical radiotherapy triggers ATM and DNA-PK$_{cs}$ activation during early DNA DSB responses and initiates a signalling cascade. While NPC relies primarily NHEJ to repair DNA DSB, GICs employ HR through ATM activation. The presence of ATMi renders G_2-checkpoint activation ineffective and prevents HR repair in GICs. Whilst allowing NPCs to compensate through NHEJ repair. GICs relatively low NHEJ activity prevents them from DNA DSB repair compensation. Consequently the ATMi treatment results in the increased cell death of GICs.

aberrant overexpression of signalling molecules in GICs that may alter DNA DSB repair. Treatment with DNA-PKi prior to irradiation did not alter Rad51 ability to resolve DNA DSB. Instead, the HR repair kinetics was similar to irradiated only samples with a return to basal levels of Rad51 foci positive cells by 24 h. The current data sets are similar to ATM knock-out cells with increased Rad51 foci accumulation post-irradiation which resulted in chromosomal abnormalities (Sun et al., 2010). The combined disruption of HR through ATMi and low NHEJ activity in GICs led to accumulation of a substantial number of unrepaired DSBs as indicated by both γH2AX and 53BP1 foci. In contrast, we found that DNA-PKi treatment had little effect on the overall DNA damage repair in GICs at early time points. The DNA-PKi treatment did, however, significantly delay NPC repair with GICs displaying better survival after DNA-PKi treatment. We showed similar data in our tumour-bearing animal model where there was no significant increase in median survival in the DNA-PKi and IR treated group. In contrast, following ATMi treatment unrepaired DSBs increased 2–3 fold in GICs while NPCs were able to survive IR-induced cell death through DNA repair mediated by the NHEJ pathway. As predicted the unrepaired DNA damage dramatically decreased GICs overall survival to a level similar to NPCs. We further demonstrated that ATMi could be employed as a potential therapy for GBM treatment, given our *in vivo* data demonstrate significant improvement in animal survival when ATMi treatment was combined with 2Gy IR. In summary, this study demonstrates that HR is an important DNA DSB repair pathway in GICs and as proof of concept, exposure to a commercially available ATMi prior to IR greatly radiosensitises GICs (Figure 6) but not non-tumourigenic NPCs. In fact, a 2Gy dose of radiation in the presence of

ATMi had a comparable effect to 10Gy IR without inhibitor treatment. Consequently targetting ATM-mediated activation of HR may provide an alternate method to increase radiosensitivity in GBM tumour without adversely affecting surrounding healthy tissue.

5. Conclusion

Clinically, most radiotherapies delivered repeated 2Gy doses over a extended period of time to minimise tissue damage while preventing recurrence (Fuller et al., 2007). Hence the *in vitro* and *in vivo* studies presented here, which use a therapeutically relevant dose of 2Gy IR in combination with ATMi define a "proof-of-principle" that targetting the HR pathway is a potential alternate treatment therapy for GBM patients. Further validation in the preclinical setting such as pharmacokinetics of the inhibitor and crossing of the blood brain barrier may be required. It may be possible to further increase the efficacy of the ATMi treatment by compounding with other inhibitors that target S-phase repair. For instance, poly-ADP ribose polymerase (PARP)-1 and -2 play a role in detecting and resolving DNA single-strand break repair. With the inclusion of PARP and ATM inhibitor, the approach will increase the rate of DNA DSBs derived from DNA SSBs during S-phase and impede the HR repair pathway, thus resulting in cellular death (Nijman and Friend, 2013). As NPCs predominantly utilise the NHEJ pathway, the drug treatment should have a radiosensitising effect on GIC while having minimal effect on surrounding normal tissue. Targeting ATM mediated activation of HR may provide an alternate method to increase radiosensitivity in aberrant stem cells derived from GBM tumour.

Funding

The above study was supported by research grants from the BrizBrain and Spinal Foundation, The University of Queensland, The National Health and Medical Research Council of Australia (GNT0631425) and The Cancer Council of Queensland (RP1042912).

Conflict of interest

The authors declare that they have no conflict of interest to disclose.

Acknowledgement

We thank Dr. Derek Richard for the pDR-GFP construct.

Appendix A. Supplementary data

Supplementary data related to this article can be found at http://dx.doi.org/10.1016/j.molonc.2014.06.012.

REFERENCES

Adams, B.R., Golding, S.E., Rao, R.R., Valer, K., 2010a. Dynamic dependence on ATR and ATM for double-strand break repair in human embryonic stem cells and neural descendants. PLoS One 5, e10001.

Adams, B.R., Hawkins, A.J., Povirk, L.F., Valerie, K., 2010b. ATM-independent, high-fidelity nonhomologous end joining predominates in human embryonic stem cells. Aging 2, 582–596.

Allen, C., Halbrook, J., Nickoloff, J.A., 2003. Interactive competition between homologous recombination and non-homologous end joining. Mol. Cancer Res. 1, 913–920.

Asaithamby, A., Chen, D.J., 2009. Cellular responses to DNA double-strand breaks after low-dose gamma-irradiation. Nucleic Acids Res. 37, 3912–3923.

Bao, S., Wu, Q., McLendon, R.E., Hao, Y., Shi, Q., Hjelmeland, A.B., Dewhirst, M.W., Bigner, D.D., Rich, J.N., 2006. Glioma stem cells promote radioresistance by preferential activation of the DNA damage response. Nature 444, 756–760.

Beamish, H., Lavin, M., 1994. Radiosensitivity in ataxia-telangiectasia: anomalies in radiation-induced cell cycle delay. Int. J. Radiat. Biol. 65, 175–184.

Beucher, A., Birraux, J., Tchouandong, L., Barton, O., Shibata, A., Conrad, S., Goodarzi, A.A., Krempler, A., Jeggo, P.A., Löbrich, M., 2006. ATM and Artemis promote homologous recombination of radiation-induced DNA double-strand breaks in G2. EMBO J 28, 3413–3427.

Brown, J.A.L., Roberts, T.L., Richards, R., Woods, R., Birrell, G., Lim, Y.C., Ohno, S., Yamashita, A., Abraham, R.T., Gueven, N., Lavin, M.F., 2011. A novel role for hSMG-1 in stress granule formation. Mol. Cell Biol. 31, 4417–4429.

Carlessi, L., Filippis, L.D., Lecis, D., Delia, A.V.D., 2006. DNA-damage response, survival and differentiation in vitro of a human neural stem cell line in relation to ATM expression. Cell Death Differ. 16, 795–806.

Clerici, M., Mantiero, D., Guerini, I., Lucchini, G., Longhese, M.P., 2008. The Yku70-Yku80 complex contributes to regulate double-strand break processing and checkpoint activation during the cell cycle. EMBO Rep. 99, 810–818.

D'Sa-Eipper, C., Roth, K.A., 2000. Caspase regulation of neuronal progenitor cell apoptosis. Dev. Neurosci. 22, 116–124.

Day, B.W., Stringer, B.W., Spanevello, M.D., Charmsaz, S., Jamieson, P.R., Ensbey, K.S., Carter, J.C., Cox, J.M., Ellis, V.J., Brown, C.L., Walker, D.G., Inglis, P.L., Allan, S., Reynolds, B.A., Lickliter, J.D., Boyd, A.W., 2011. ELK4 neutralization sensitizes glioblastoma to apoptosis through downregulation of the anti-apoptotic protein Mcl-1. Neuro Oncol 13, 1202–1212.

Day, B.W., Stringer, B.W., Al-Ejeh, F., Ting, M.J., Wilson, J., Ensbey, K.S., Jamieson, P.R., Bruce, Z.C., Lim, Y.C., Offenhäuser, C., Charmsaz, S., Cooper, L.T., Ellacott, J.K., Harding, A., Leveque, L., Inglis, P., Allan, S., Walker, D.G., Lackmann, M., Osborne, G., Khanna, K.K., Reynolds, B.A., Lickliter, J.D., Boyd, A.W., 2013. EphA3 maintains tumorigenicity and is a therapeutic target in glioblastoma multiforme. Cancer Cell 23, 238–248.

Donato, R., Miljan, E.A., Hines, S.J., Aouabdi, S., Pollock, K., Patel, S., Edwards, F.A., Sinden, J.D., 2007. Differential development of neuronal physiological responsiveness in two human neural stem cell lines. BMC Neurosci. 8, 36–47.

Escribano-Díaz, C., Orthwein, A., Fradet-Turcotte, A., Xing, M., Young, J.T.F., Tkáč, J., Cook, M.A., Rosebrock, A.P., Munro, M., Canny, M.D., Xu, D., Durocher, D., 2013. A cell cycle-dependent regulatory circuit composed of 53BP1-RIF1 and BRCA1-CtIP controls DNA repair pathway choice. Mol. Cell 49, 872–883.

Fluckiger, A.-C., Marcy, G., Marchand, M., Négre, D., Cosset, F.-L., Mitalipov, S., Wolf, D., Savatier, P., Dehay, C., 2005. Cell cycle

features of primate embryonic stem cells. Stem Cells 24, 547–556.
Franken, N., Rodermond, H., Stap, J., Haveman, J., Bree, C.V., 2006. Clonogenic assay of cells in vitro. Nat. Protoc. 1, 2315–2319.
Fuller, C.D., Choi, M., Forthuber, B., Wang, S.J., Rajagiriyil, N., Salter, B.J., Fuss, M., 2007. Standard fractionation intensity modulated radiation therapy (IMRT) of primary and recurrent glioblastoma multiforme. Radiat. Oncol. 2, 26–33.
Goodarzi, A.A., Yu, Y., Riballo, E., Douglas, P., Walker, S.A., Ye, R., Härer, C., Marchetti, C., Morrice, N., Jeggo, P.A., Lees-Miller, S.P., 2006. DNA-PK autophosphorylation facilitates Artemis endonuclease activity. EMBO J 25, 3880–3889.
Hickson, I., Zhao, Y., Richardson, C.J., Green, S.J., Martin, N.M.B., Orr, A.I., Reaper, P.M., Jackson, S.P., Curtin, N.J., Smith, G.C.M., 2004. Identification and characterization of a novel and specific inhibitor of the ataxia-telangiectasia mutated kinase ATM. Cancer Res. 64, 9152–9159.
Hosoya, N., Miyagawa, K., 2009. Clinical importance of DNA repair inhibitors in cancer therapy. MEMO 2, 9–14.
Huertas, P., Jackson, S.P., 2009. Human CtIP mediates cell cycle control of DNA end resection and double strand break repair. J. Biol. Chem. 284, 9558–9565.
Karanjawalaa, Z.E., Adachia, N., Irvinea, R.A., Oha, E.K., Shibataa, D., Schwarzb, K., Hsieha, C.-L., Lieber, M.R., 2002. The embryonic lethality in DNA ligase IV-deficient mice is rescued by deletion of Ku: implications for unifying the heterogeneous phenotypes of NHEJ mutants. DNA Repair 1, 1017–1026.
Katayama, K., Ueno, M., Yamauchi, H., Nagata, T., Nakayama, H., Doi, K., 2005. Ethylnitrosourea induces neural progenitor cell apoptosis after S-phase accumulation in a p53-dependent manner. Neurobiol. Dis. 18, 218–225.
Langerak, P., Mejia-Ramirez, E., Limbo, O., Russell, P., 2011. Release of Ku and MRN from DNA ends by Mre11 nuclease activity and Ctp1 is required for homologous recombination repair of double-strand breaks. PLoS Genet. 7, e1002271.
Lavin, M.F., 2008. Ataxia-telangiectasia: from a rare disorder to a paradigm for cell signalling and cancer. Nat. Rev. Mol. Cell Biol. 9, 759–769.
Li, X., Heyer, W.-D., 2008. Homologous recombination in DNA repair and DNA damage tolerance. Cell Res. 18, 99–113.
Lim, Y.C., Roberts, T.L., Day, B.W., Harding, A., Kozlov, S., Kijas, A.W., Ensbey, K.S., Walker, D., Lavin, M.F., 2012. A role for homologous recombination and abnormal cell-cycle progression in radioresistance glioma-initiating cells. Mol. Cancer Ther. 11, 1863–1872.
Limbo, O., Chahwan, C., Yamada, Y., Bruin, R.A.d, Wittenberg, C., Rusell, P., 2007. Ctp1 is a cell-cycle-regulated protein that functions with Mre11 complex to control double-strand break repair by homologous recombination. Mol. Cell 28.
Loeffler, J.S., Alexander 3rd, E., Shea, W.M., Wen, P.Y., Fine, H.A., Kooy, H.M., Black, P.M., 1992. Radiosurgery as part of the initial management of patients with malignant gliomas. J. Clin. Oncol. 10, 1379–1385.
Lomonaco, S.L., Finniss, S., Xiang, C.L., DeCarvalho, A., Umansky, F., Kalkanis, S.N., Mikkelsen, T., Brodie, C., 2009. The induction of autophagy by gamma-radiation contributes to the radioresistance of glioma stem cells. Int. J. Cancer 3, 717–722.
Mao, Z., Bozzella, M., Seluanov, A., Gorbunova, V., 2008. DNA repair by nonhomologous end joining and homologous recombination during cell cycle in human cells. Cell Cycle 7, 2902–2906.
Meador, J.A., Su, Y., Ravanat, J.-L., Balajee, A.S., 2010. DNA-dependent protein kinase (DNA-PK)-deficient human glioblastoma cells are preferentially sensitized by Zebularine. Carcinogenesis 31, 184–191.
Meletis, K., Wirta, V., Hede, S.-M., Nistér, M., Lundeberg, J., Frisén, J., 2006. p53 suppresses the self-renewal of adult neural stem cells. Development 133, 363–369.
Nicolette, M.L., Lee, K., Guo, Z., Rani, M., Chow, J.M., Lee, S.E., Paull, T.T., 2010. Mre11–Rad50–Xrs2 and Sae2 promote 5′ strand resection of DNA double-strand breaks. Nat. Struct. Mol. Biol. 17, 1478–1485.
Nijman, S.M.B., Friend, S.H., 2013. Potential of the synthetic lethality principle. Science 342, 809–811.
Patel, A.G., Sarkaria, J.N., Kaufmann, S.H., 2011. Nonhomologous end joining drives poly(ADP-ribose) polymerase (PARP) inhibitor lethality in homologous recombination-deficient cells. Proc. Natl. Acad. Sci. U S A 108, 3406–3411.
Reynolds, B.A., Weiss, S., 1992. Generation of neurons and astrocytes from isolated cells of the adult mammalian central nervous system. Science 255, 1707–1710.
Roberts, T.L., Ho, U., Luff, J., Lee, C.S., Apte, S.H., MacDonald, K.P., Raggat, L.J., Pettit, A.R., Morrow, C.A., Waters, M.J., Chen, P., Woods, R.G., Thomas, G.P., St Pierre, L., Farah, C.S., Clarke, R.A., Brown, J.A., Lavin, M.F., 2013. Smg1 haploinsufficiency predisposes to tumor formation and inflammation. Proc. Natl. Acad. Sci. U S A 110, E285–E294.
Sak, A., Stueben, G., Groneberg, M., Böcker, W., Stuschke, M., 2005. Targeting of Rad51-dependent homologous recombination: implications for the radiation sensitivity of human lung cancer cell lines. Br. J. Cancer 92, 1089–1097.
Sanai, N., Berger, M.S., 2008. Glioma extent of resection and its impact on patient outcome. Neurosurgery 62, 753–766.
Sarkaria, J.N., Tibbetts, R.S., Busby, E.C., Kennedy, A.P., Hill, D.E., Abraham, R.T., 1998. Inhibition of phosphoinositide 3-kinase related kinases by the radiosensitizing agent wortmannin. Cancer Res. 58, 4375–4382.
Short, S.C., Giampieri, S., Worku, M., Alcaide-German, M., Sioftanos, G., Bourne, S., Lio, K.I., Shaked-Rabi, M., Martindale, C., 2011. Rad51 inhibition is an effective means of targeting DNA repair in glioma models and CD133+ tumor-derived cells. Neuro Oncol. 13, 487–499.
Short, S.C., Martindale, C., Bourne, S., Brand, G., Woodcock, M., Johnston, P., 2007. DNA repair after irradiation in glioma cells and normal human astrocytes. Neuro Oncol. 9, 404–411.
Siegel, R., DeSantis, C., Virgo, K., Stein, K., Mariotto, A., Smith, T., Cooper, D., Gansler, T., Lerro, C., Fedewa, S., Lin, C., Leach, C., Cannady, R.S., Cho, H., Scoppa, S., Hachey, M., Kirch, R., Jemal, A., Ward, E., 2012. Cancer treatment and survivorship statistics, 2012. CA Cancer J. Clin. 62, 220–241.
Singh, S.K., Clarke, I.D., Terasaki, M., Bonn, V.E., Hawkins, C., Squire, J., Dirks, P.B., 2003. Identification of a cancer stem cell in human brain tumors. Cancer Res. 63, 5821–5828.
Sirbu, B.M., Lachmayer, S.J., Wülfing, V., Marten, L.M., Clarkson, K.E., Lee, L.W., Gheorghiu, L., Zou, L., Powell, S.N., Dahm-Daphi, J., Willers, H., 2011. ATR-p53 restricts homologous recombination in response to replicative stress but does not limit DNA interstrand crosslink repair in lung cancer cells. PLoS One 6, e23053.
Sturgeon, C.M., Knight, Z.A., Shokat, K.M., Roberge, M., 2006. Effect of combined DNA repair inhibition and G2 checkpoint inhibition on cell cycle progression after DNA damage. Mol. Cancer Ther. 5, 885–892.
Sun, J., Oma, Y., Harata, M., Kono, K., Shima, H., Kinomura, A., Ikura, T., Suzuki, H., Mizutani, S., Kanaar, R., Tashir, S., 2010. ATM modulates the loading of recombination proteins onto a chromosomal translocation breakpoint hot spot. PLoS One 5, e13554.
Takata, M., Sasaki, M.S., Sonoda, E., Morrison, C., Hashimoto, M., Utsumi, H., Yamaguchi-Iwai, Y., Shinohara, A., Takeda, S., 1998. Homologous recombination and non-homologous end-joining pathways of DNA double strand break repair have overlapping roles in the maintenance of chromosomal integrity in vertebrate cells. EMBO J 17, 5497–5508.

Tamura, K., Aoyagi, M., Wakimoto, H., Ando, N., Nariai, T., Yamamoto, M., Ohno, K., 2010. Accumulation of CD133-positive glioma cells after high-dose irradiation by Gamma knife surgery plus external beam radiation. J. Neurosurg. 113, 310–318.

Tang, J., Cho, N.W., Cui, G., Manion, E.M., Shanbhag, N.M., Botuyan, M.V., Mer, G., Greenberg, R.A., 2013. Acetylation limits 53BP1 association with damaged chromatin to promote homologous recombination. Nat. Struct. Mol. Biol. 20, 317–325.

Terry, N.H.A., White, R.A., 2006. Flow cytometry after bromodeoxyuridine labeling to measure S and G2+M phase durations plus doubling times in vitro and in vivo. Nat. Protoc. 1, 859–869.

Tichy, E.D., Pillai, R., Deng, L., Liang, L., Tischfield, J., Schwemberger, S.J., Babcock, G.F., Stambrook, P.J., 2010. Mouse embryonic stem cells, but not somatic cells, predominantly use homologous recombination to repair double-strand DNA breaks. Stem Cells Dev. 19, 1699–1711.

Tsuzuki, T., Fujii, Y., Sakumi, K., Tominaga, Y., Nakao, K., Sekiguchi, M., Matsushiro, A., Yoshimura, Y., Morita, T., 1996. Targeted disruption of the Rad51 gene leads to lethality in embryonic mice. Proc. Natl. Acad. Sci. U S A 93, 6236–6240.

Wang, H., Wang, X., Iliakis, G., Wang, Y., 2003. Caffeine could not efficiently sensitize homologous recombination repair-deficient cells to ionizing radiation-induced killing. Radiat. Res. 159, 420–425.

Weller, M., Cloughesy, T., Perry, J.R., Wick, W., 2013. Standards of care for treatment of recurrent glioblastoma–are we there yet? Neuro Oncol. 15, 4–27.

Xu, B., Kim, S.-T., Lim, D.-S., Kastan, M.B., 2002. Two molecularly distinct G2/M checkpoints are induced by ionizing irradiation. Mol. Cell Biol. 22, 1049–1059.